Int. J. Electrochem. Sci., 7 **(2012)** 12391 - 12403

International Journal of
ELECTROCHEMICAL
SCIENCE
www.electrochemsci.org

H_2S Corrosion Inhibition of Carbon Steel by a Coconut-Modified Imidazoline

L.M. Rivera-Grau[1], *M. Casales*[2], *I. Regla*[2,3], *D. M. Ortega-Toledo*[2], *J.A. Ascencio-Gutierrez*[2], *J.G. Gonzalez-Rodriguez*[1,*], *L. Martinez-Gomez*[2]

[1] Universidad Autonoma del Estado de Morelos, CIICAp, AV. Universidad 1001, 62209-Cuernavaca, Mor., Mexico

[2] Universidad Nacional Autonoma de Mexico, Instituto de Ciencias Fisicas, AV. Universidad s/n, Cuernavaca, Mor., Mexico

[3] Universidad Nacional Autonoma de Mexico, Facultad de Estudios Superiores Zaragoza, Mexico D.F., Mexico

[*]E-mail: ggonzalez@uaem.mx

Received: 24 September 2012 / *Accepted:* 31 October 2012 / *Published:* 1 December 2012

A coconut oil-modified imidazoline, namely aminoehtyl-amine imidazoline, was prepared as green corrosion inhibitor to investigate the H_2S corrosion inhibition behavior of 1018 carbon steel and compared with a commercial hydroxyetyl-imidazoline. Techniques included polarization curves, linear polarization curves, electrochemical impedance and electrochemical noise measurements with inhibitor concentrations of 25 ppm. It was found that the coconut oil-modified imidazoline had a better corrosion inhibition performance than the commercial one, decreasing the corrosion rate by one order of magnitude and giving promising results in the preparation of green corrosion inhibitors.

Keywords: Green inhibitor, acidic corrosion, carbon steel

1. INTRODUCTION

Oilfield corrosion manifests itself in several forms, among which CO_2 corrosion (sweet corrosion) and hydrogen sulfide (H_2S) corrosion (sour corrosion) in the produced fluids and corrosion by oxygen dissolved in water injection are by far the most prevalent forms of attack found in oil and gas production [1]. Because of its implications in different industries, the corrosion of steel in H_2S-containing solutions is a well-known phenomenon that has been investigated during many years [2]. The presence of H_2S and CO_2 and impurities such as chlorides, cyanides, etc… promotes the corrosion phenomenon. In the literature, there are studies of the effect of H_2S concentration on steel [3],and iron [4], the effect of Cl^- on steel [5], the effect of Cl^- and H_2S on steel weld [6]. The results demonstrated that H_2S could accelerate both the anodic iron dissolution and the cathodic hydrogen

evolution in most cases [7-10], but some results showed that H_2S could also inhibit the corrosion of iron under certain special conditions [11,12].

The injection of corrosion inhibitor is a standard practice in oil and gas production systems to control internal corrosion of carbon steel structures. Nitrogen-based organic inhibitors, such as imidazolines or their salts have been successfully used in these applications even without an understanding of the inhibition mechanism [13-15]. The corrosion inhibition of organic compounds is related to their adsorption properties. Adsorption depends on the nature and the state of the metal surface, on the type of corrosive environment and on the chemical structure of the inhibitor [13]. Different derivatives from imidazolines are employed as steel corrosion inhibitors. Even though they have been specially employed in the oil industry, only recently a respectable amount of studies have been undertaken to understand how they work. [9,14-20]. These inhibitors are evaluated in field conditions or simulated media by weight loss measurements, which do not reflect the changes experienced by the corrosion mechanism whatsoever. Related studies have used electrochemical techniques such as potentiodynamic techniques, electrochemical impedance spectroscopy and open circuit potential measurements, which show significant changes in the corrosion due to the presence of inhibitors [21-24].

Recently Yoo et al. [25] evaluated a bio-diesel-based imidazoline, namely 2-(2-alkyl-4,5-dihydro-1H-imidazol-1-yl)ethanol, as corrosion inhibitor of mild steel in 1.0 M hydrochloric acid (HCl) and compared with the same imidazoline but prepared with petroleum-based chemicals. It was found that when the bio-diesel-based imidazoline had a concentration over 100 ppm, it acted as an effective corrosion inhibitor. An undergoing research project in our laboratory deals with the possibility of using coconut oil as corrosion inhibitors. Thus, the aim of this work is to evaluate the corrosion inhibition performance of a coco-modified imidazoline in an H_2S-containing environment.

2. EXPERIMENTAL

Material tested was a 1018 carbon steel cylinder measuring 25 mm in length and 5.0 mm diameter. Before testing, the electrode was polished to 600 grit SIC emery paper and then cleaned with alcohol, acetone and distilled water. Inhibitors used in this work include a commercial hydroxyetyl-imidazoline (inhibitor A) and an aminoehtyl-amine imidazoline, (inhibitor B) which resulted from modifying inhibitor A with coconut. The general structure of both inhibitors is shown on Fig. 1. A mixture of distilled coconut biodiesel (59-120 ° C / 0.05 mmHg) 2.22 g and 0.936 g of 2-(2-aminoethylamino)ethanol were heated and magnetically stirred at 140 ° C during 9 hours at atmospheric pressure and 3 hours at a reduced pressure (20 mm Hg). The reaction mixture was distilled at the Kugelrohr apparatus under reduced pressure (235 ° C /0.05 mmHg) to obtain 1.42 g of coconut imidazoline mixture. Inhibitors were dissolved in pure 2-propanol. The concentration of the inhibitors used in this work was 25 ppm and the temperature kept at 50°C. The testing solution consisted of 3% NaCl solution, heated, de-aerated with nitrogen gas, and H_2S was produced by reacting Sodium Sulfide (Na_2S) with Acetic acid. Inhibitor was added 2 hours after pre-corroding the specimen.

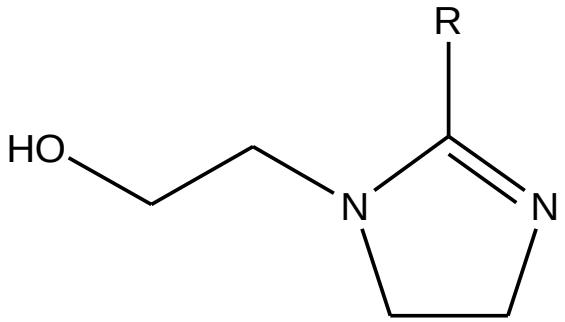

Figure 1. General structure of hydroxyethyl imidazoline, where R is an alkyl chain derivative.

Electrochemical techniques employed included poltenthiodynamic polarization curves, linear polarization resistance, LPR, and electrochemical impedance spectroscopy, EIS, and electrochemical noise, EN, measurements. Polarization curves were recorded at a constant sweep rate of 1 mV/s and the scanning range was from -300 to +300 mV respect to the open circuit potential, E_{corr}. Measurements were obtained by using a conventional three electrodes glass cell with two graphite electrodes symmetrically distributed and a saturated calomel electrode (SCE) as reference with a Lugging capillary bridge. Inhibition efficiencies (*E(%)*) were determined from the corrosion current densities calculated by the Tafel extrapolation method according to the following equation

$$E(\%) = \frac{i_i - i_b}{i_i} \text{ X } 100 \qquad (1)$$

where i_b is the corrosion rate without inhibitor and i_i the corrosion rate in the solution with inhibitor. LPR measurements were carried out by polarizing the specimen from +10 to –10 mV respect to E_{corr}, at a scanning rate of 1 mV/s. Inhibition efficiencies [*E(%)]* were determined according to the following equation:

$$E(\%) = \frac{R_{p,i} - R_{p,b}}{R_{p,i}} \text{ X } 100 \qquad (2)$$

where $R_{p,b}$ is the linear polarization resistance without inhibitor and $R_{p,i}$ is the linear polarization resistance with inhibitor. Electrochemical impedance spectroscopy tests were carried out at E_{corr} by using a signal with an amplitude of 10 mV and a frequency interval of 0.1-100KHz. An ACM potentiostat controlled by a desk top computer was used for the LPR tests and polarization curves, whereas for the EIS measurements, a model PC4 300 Gamry potentiostat was used. Finally, EN measurements for both current and potential were recorded using two identical working electrodes and a saturated calomel reference electrode (SCE). Electrochemical noise measurements were carried out by simultaneously recording potential and current fluctuations at a sampling rate of 1 point per second for a period of 1024 seconds. A fully automated zero resistance ammeter (ZRA) from ACM instruments was used in this case. Removal of the DC trend from the raw noise data was the first step in the noise analysis. To accomplish this, a least square fitting method was used. Finally, noise

resistance, R_n, was then calculated as the ratio of potential noise standard deviation, σ_v, over current noise standard deviation, σ_i.

3. RESULTS AND DISCUSSION

The effect of inhibitors A and B on the polarization curves in the H_2S-containing 3% NaCl solution at 50°C is shown in Fig. 2.

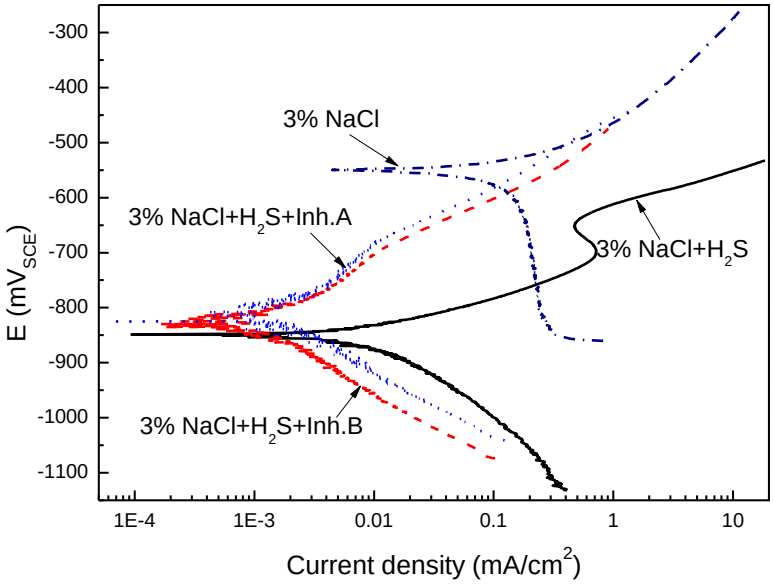

Figure 2. Effect of inhibitors A and B on the polarization curves in the H_2S-containing 3% NaCl solution at 50°C.

For comparison, the polarization curve for pure 3%NaCl solution is shown. It can be seen that the curve for pure 3% NaCl solution shows the noblest E_{corr} value, -550 mV, and the highest corrosion current density value, i_{corr}, around 0.16 mA/cm^2. The anodic branch does not show the presence of a passive layer but only anodic dissolution, however, a limiting current density can be seen in the cathodic branch due to the oxygen reduction reaction. When H_2S is present, the E_{corr} value is made more cathodic, reaching a value close to -850 mV and the i_{corr} value is decreased for more than one order of magnitude, reaching a value close to 0.01 mA/cm^2, where the inhibiting effect of H_2S reported previously can be seen [11,12] which has been attributed to the presence of a thin layer of Fe_2S. It can be seen that both branches of the polarization curves are modified, since in the cathodic side a narrow passive region can be seen between -680 and -630 mV whereas the cathodic limiting current density does not appear this time. As soon as both inhibitors are added to the H_2S-containing 3% NaCl solution, the E_{corr} values attained more positive values than that for the blank solution, implying that both inhibitors act as anodic-type inhibitor; the anodic and cathodic current density values are decreased, being more pronounced the effect in the anodic branch, where the current density were

lowered by more than one order of magnitude. The i_{corr} values reached values close to 0.0017 and 0.0011 mA/cm^2 for inhibitors A and B respectively, more than one order of magnitude lower than those without inhibitor. These values are reported in table 1.

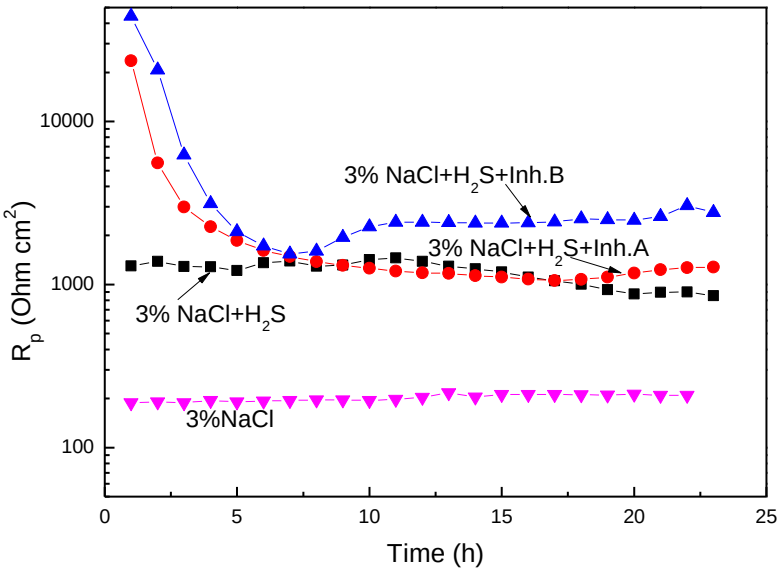

Figure 3. Effect of inhibitors A and B on the change of the R_p value with time in the H_2S-containing 3% NaCl solution at 50°C.

Table 1. Electrochemical parameters obtained from the polarization curves.

Solution	E_{corr} (mV_{SCE})	i_{corr} (mA/cm^2)
3% NaCl	-550	0.16
3% NaCl+H_2S	-850	0.011
3% NaCl+H_2S+ inh. A	-820	0.0017
3% NaCl+H_2S+ inh. B	-834	0.0011

The change in the polarization resistance value with time, R_p, for the different solutions is shown in Fig. 3. This figure shows that, as the polarization curves indicated, the lowest R_p value, and thus the highest corrosion rate, was obtained for the 3% NaCl solution. For uninhibited H_2S-containing solution, the obtained R_p values were almost one order of magnitude higher than the pure 3% NaCl solution during the whole test, showing, again, the inhibitory effect of the H_2S, showing the stability of protective Fe_2S film on the steel surface. When either inhibitor A or B were added to the 3% NaCl+H_2S solution, the R_p increased for more than one order of magnitude, decreasing the corrosion rate, but after 5 hours or so, the R_p values decreased reaching values very similar to those obtained with the uninhibited 3% NaCl+H_2S solution, although for inhibitor B, the R_p values were two times higher than those obtained with the uninhibited solution.

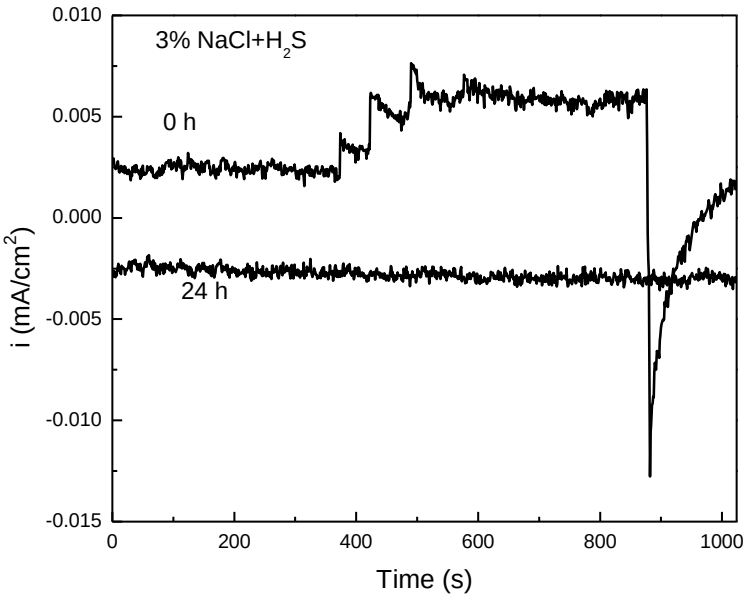

Figure 4. Noise in current for carbon steel exposed to the H_2S-containing 3% NaCl solution at 50°C at different exposure times.

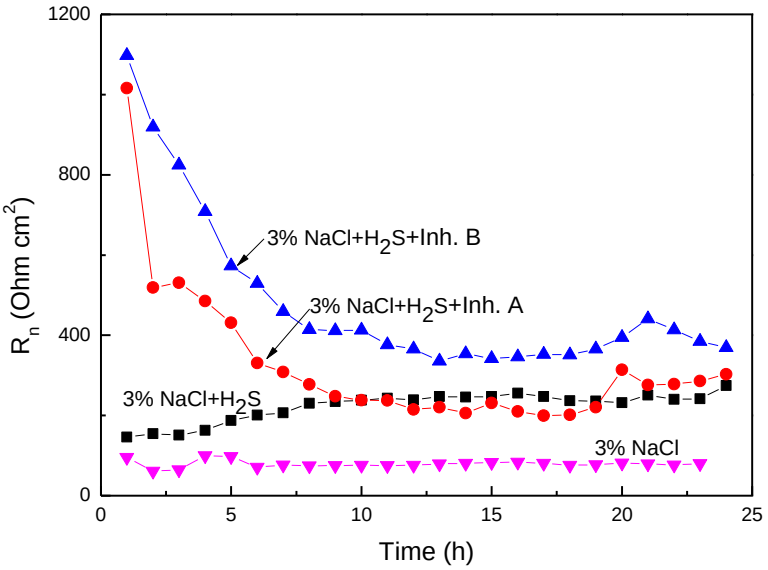

Figure 5. Effect of inhibitors A and B on the change of the R_n value with time in the H_2S-containing 3% NaCl solution at 50°C.

As an example of the electrochemical noise readings, Fig. 4 shows the time series for the noise in current measurements in the 3% NaCl+H_2S solution at the beginning of the experiment and after 24 hours of testing. Time series at the beginning of the experiment shows transients of low intensity and high frequency, typical of a material undergoing uniform type of corrosion, together with some transients with a sudden increase in intensity and a slow decay with low frequency are present, which

are typical of a localized type of corrosion. According to [26], an increase in current is attributed either to film rupture or to pit nucleation, while the subsequent decrease in current is attributed to the recovery of a passive film without pit propagation and indicates a tendency towards localized corrosion. By using the ratio of the potential noise standard deviation, σ_v, over current noise standard deviation, σ_i, the noise resistance, R_n, was calculated and the results are shown in Fig. 5. This figure shows that the lowest R_n value corresponds to the pure 3% NaCl solution with a value which remains constant throughout the experiment. When H_2S is added to this solution, the R_n value slightly increased as compared to that for the 3% NaCl solution and kept increasing in a slow fashion. However, when both inhibitors were added to the system, the R_n increased for more than one order of magnitude, reaching the highest value with the addition of inhibitor B. However, the R_n value for both inhibitors decreased rapidly reaching a steady state value around 9 hours or so. For inhibitor A the steady state R_n value was the same as that for uninhibited 3% NaCl+H_2S solution, but that for inhibitor B was slightly higher. If we compare the behavior of R_n from Fig. 5 and that for R_p from Fig. 4 we can see that is very similar, which is very encouraging, since similar results are obtained by using different techniques.

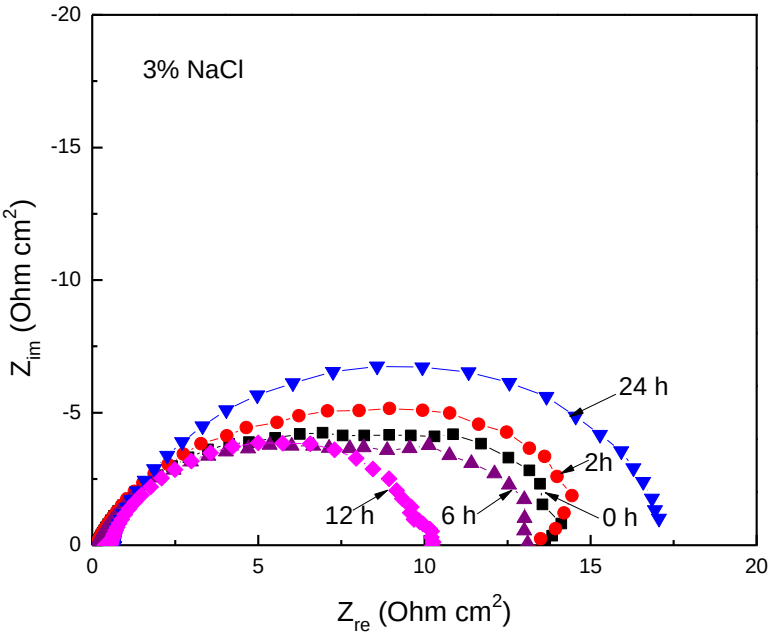

Figure 6. Nyquist diagrams for carbon steel exposed to a 3% NaCl solution at 50°C.

Niquist diagrams for the 3% NaCl solution during the 24 hours of testing are shown in Fig. 6 which shows at all times depressed capacitive-like semicircles, with their centers in the real axis, indicating that the corrosion process is under charge transfer control from the metal to the electrolyte through the double electrochemical layer. The semicircle diameter practically remained the same throughout the test, around 15 ohm cm^2.

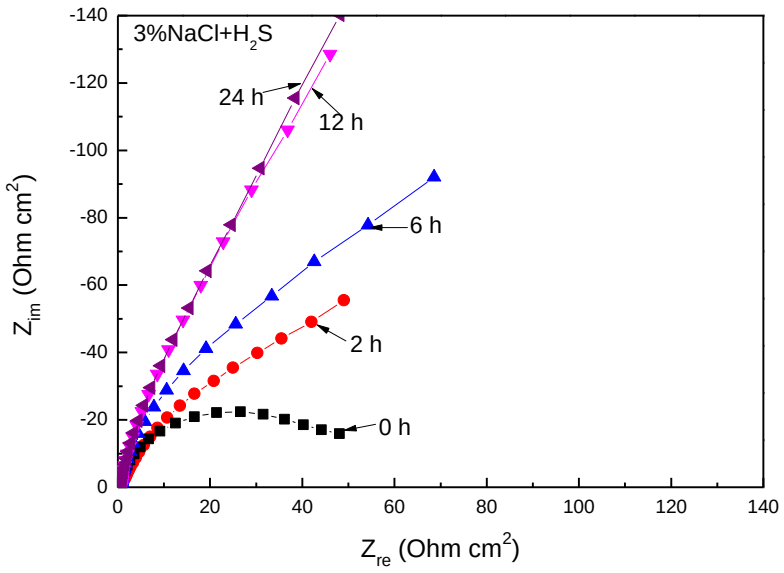

Figure 7. Nyquist diagrams for carbon steel exposed to a 3% NaCl + H_2S solution at 50°C.

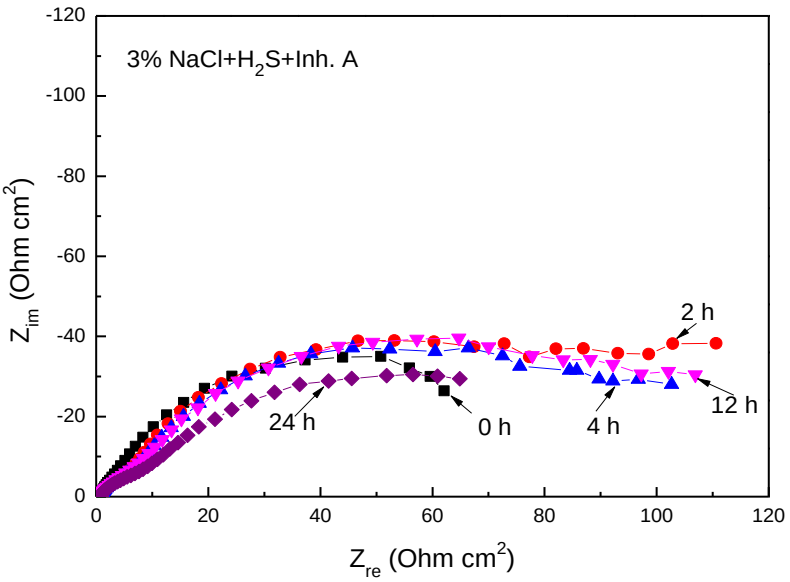

Figure 8. Nyquist diagrams for carbon steel exposed to a 3% NaCl + H_2S + inhibitor A solution at 50°C.

However, when H_2S was added to the solution, Fig. 7, the semicircle diameter was higher than that obtained with pure 3% NaCl solution, obtaining its lowest value at the beginning of the experiment, around 50 ohm $cm^2$and kept increasing as time elapsed reaching its highest value after 24 hours of testing. When inhibitor A was added to the system, Fig. 8, Nyquist data describe a single depressed, capacitive-like semicircle at all frequencies at the beginning of the test, but after 2 hours

there are two semicircles, one at high and intermediate frequencies and a second one at lower frequency values.

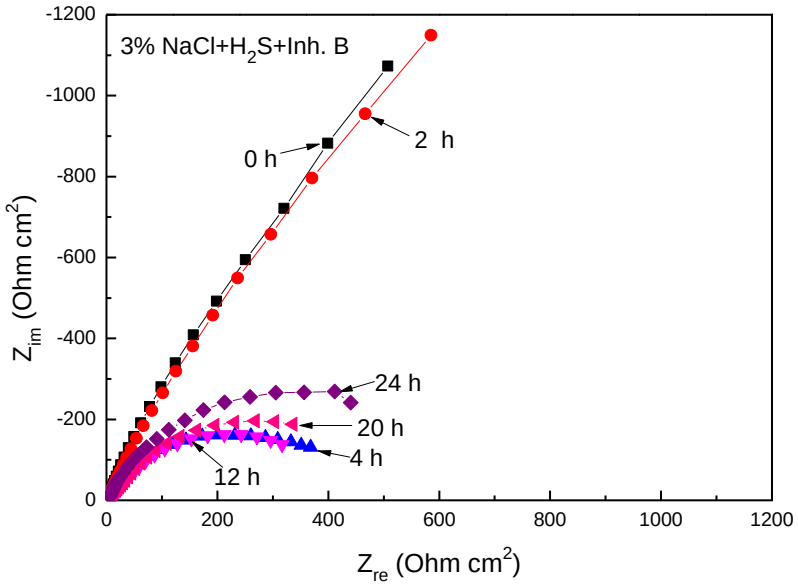

Figure 9. Nyquist diagrams for carbon steel exposed to a 3% NaCl + H_2S + inhibitor B solution at 50°C.

The real impedance remained more or less constant throughout the tests and is similar to that found for uninhibited 3% NaCl+H_2S solution, Fig. 7. The first semicircle can be attributed to the double electrochemical layer, whereas the second one has been attributed to the presence of a complex formed by the corrosion products land the inhibitor.

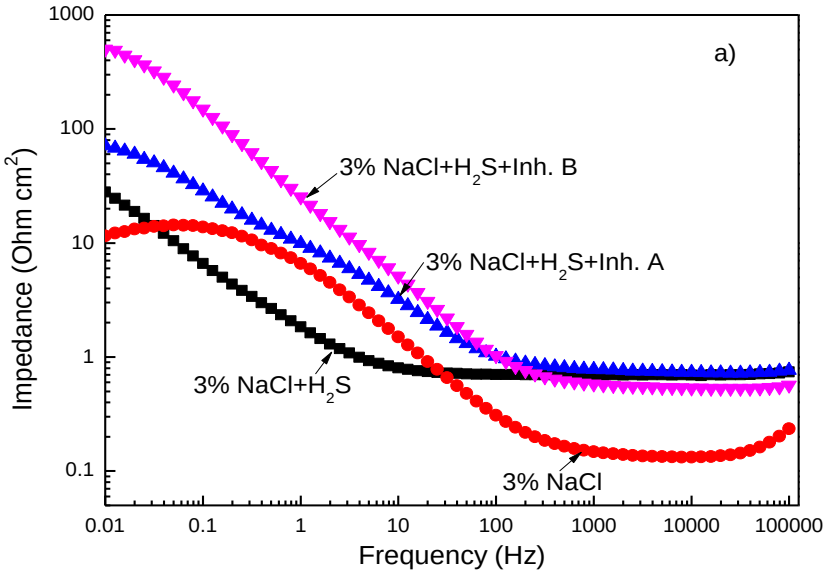

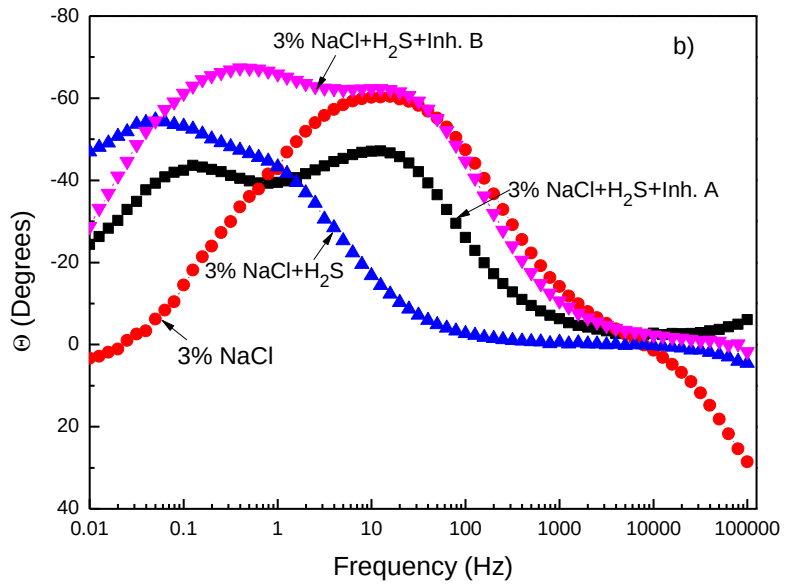

Figure 10. Bode diagrams in the a) impedance and b) Phase format for carbon steel exposed to different H_2S-3% NaCl solutions.

When inhibitor B was added, Fig. 9, Nyquist diagrams show that the data describe a single depressed capacitive-like semicircle with its centre in the real axis. During the first hours of testing, the semicircle diameter is much higher to that found for uninhibited 3% NaCl+H_2S solution or for the solution with the addition of inhibitor A for at least one order of magnitude, but this value decreases as time elapses. However, the final semicircle diameter obtained with inhibitor B was higher than that obtained with inhibitor A, indicating a much better performance of inhibitor B, the coco-modified one.

Fig. 10 shows Bode diagrams in both impedance and phase angle formats for all the tested solutions at the beginning of the experiment. Impedance plots, Fig. 10 a, show that the lowest impedance or modulus corresponds to the 3% NaCl solution, followed by the uninhibited 3% NaCl+H_2S solution, whereas the highest value, more than one order of magnitude, was obtained with the addition of inhibitor B. On the other hand, Bode diagrams in the phase angle format, Fig. 10 b, shows the presence of only one peak for the 3% NaCl solution, whereas uninhibited 3% NaCl+H_2S solution seems to show two peaks at 0.1 and 1.0 Hz, but either with the addition of inhibitors A or B there are two well defined peaks at 10 and 1.0 Hz. The presence of two peaks indicates the formation of a protective corrosion products layer.

As discussed in previous works [27, 28], the effects of H_2S on the carbon steel corrosion can be summarized as follows: i) formation of iron sulfide (FeS) films, ii) an additional effect of H_2S reduction and iii) an additional contribution to the anodic dissolution of iron, which is mediated by the adsorption of HS^- ions. These three effects account for the dependence of the corrosion rate of iron on the presence of H_2S. The semicircle formed in the complex plane plots, Figs. 4-6, could possibly be attributed to the charge transfer process given by the following reactions:

Anodic reaction:

$$Fe \rightarrow Fe^{2+} + 2e^{-} \quad (3)$$

Cathodic reaction:

$$H_2S_{(aq)} + 2e^{-} \rightarrow S^{2-} + H_2 \quad (4)$$

Overall reaction:

$$Fe + H_2S_{(aq)} \rightarrow FeS + H_2 \quad (5)$$

The corrosion mechanism of carbon steel immersed in the H_2S-containing 3 % wt. NaCl solution involves the growth of an iron sulfide film on carbon steel from the outward migration of iron atoms and subsequent dissolution of the sulfide film at the metal-solution interface. In the Nyquist plots shown in Figs. 4-6, a process is occurring i.e. charge transfer at the metal/corrosion products and corrosion products/solution interfaces involving the oxidation of iron and the reduction of hydrogen ions.

The film which is formed is a non-adherent layer, which can be easily removed from the steel surface and can not passivate the steel. This explains the results given by polarization curves (Fig. 2) and Nyquist diagrams (Figs. 6-9). Some particles, like carbides, nitrides, etc… can act as cathodic sites and form micro galvanic cells with the rest of the steel, which will act as anode. In addition, the presence of these particles represent heterogeneities on the surface and act as sites for the disruption of any film present on the surface and, therefore, the start of localized corrosion such as pitting. This could explain the presence of the transients observed on the instantaneous noise resistance readings, Figs.4-5. The molecular structure of hydroxyethyl imidazoline, Fig. 1, is composed of a five member ring containing nitrogen elements, a C-14 saturated hydrophobic head group and a pendant, hydrophilic hydroxyethyl group attached to one of the nitrogen atoms. The compound can be adsorbed on the metal surface by the formation of an iron-nitrogen co-ordination bond and by a pi-electron interaction between the pi-electron in the head group and iron [10-12]. Though not a primary contribution to the adsorption strength of the compound on the surface of the metal, coulombic attraction between the negative charge, i.e. electrons, on the metal surface (as a result of the specific adsorption of chloride ions) and the imidazoline derivative may also contribute to the inhibition ability of the compound. When the adsorbed inhibitor molecules exceed certain number of atoms on the surface and these molecules are close enough, electrostatic repulsion between the negative charge of the pendant group, leads to a desorption of the inhibitor molecules, leading to unprotected sites on the metal and an increase on the corrosion rate. The fact that the coconut-modified imidazoline has a similar, or even a better corrosion performance that the commercial one is very encouraging because provides very promising results in the preparation of green corrosion inhibitors.

4. CONCLUSIONS

A commercial imidazoline-base corrosion inhibitor has been modified with coconut oil and its corrosion inhibition performance for carbon steel in acidic solution. It was found with different techniques that even with small concentrations such as 20 ppm the corrosion inhibition of the commercial imidazoline-based inhibitor are improved by the modification with vegetable oil. This indicates that small doses of coconut-modified imidazoline could be used as a corrosion inhibitor. The p-electrons of double bonds interacted with the d-orbitals of the atoms on the metal surface, and the unshared electron pair-containing nitrogen enhanced the adsorption of the modified imidazoline on the metal surface, resulting in the formation of a relatively stable barrier against corrosion.

ACKNOWLEDGEMENTS
The authors acknowledge D. Cuervo and DGAPA-UNAM for Ignacio Regla sabbatical fellowship at ICF-UNAM.

References

1. M.B. Kermani, A. Morshed, *Corrosion* 59 (8) (2003) 659
2. S.N. Smith, "A Proposed Mechanism for Corrosion in Slightly Sour Oil and Gas Production". Poc. 12th Int. Corrosion Congress held in September 19-23 1993 (Houston, TX: NACE International 1993)
3. S. Arzola, J. Genesca , *J. Solid State Electrochem*., 8 (2005), pp. 197–200
4. H.Y. Ma, X.L. Cheng, S.H. Chen, G.Q. Li, X. Chen, S.B. Lei, H.Q. Yang, *Corrosion*, 54 (1998), pp. 634–640
5. Y.S. Choi, J.G. Kim, *Corrosion*, 56 (2000), pp. 1202–1210
6. H.H. Huang, W.T. Tsai, J.T. Lee , *Mater. Sci. Eng*. A, 188 (1994), pp. 219–227
7. V. Jovancicevic, S. Ramachandran and P. Prince, *Corrosion* 55 (1999) 449
8. Ramachandran S and Jovancicevic V., *Corrosion* 55 (3) (1999) 259
9. Z. Xueyuan, Corrosion Science 43 (2001) 1417
10. F. Bentiss, M. Lagrenee, M. Traisnel, J.C. Hornez, *Corros. Sci*. 41, (1999) 789.
11. S. Ramachandran, M. Tsai, M. Blanco, H. Chen, W. A. Tang, Godard III *Langmuir* 12 (1996) 6419.
12. D. Wang, S. Li, M. Ying, M. Wang, Z. Xiao, Z. Chen, *Corros. Sci*, 41 (1999) ; 1911.
13. F. Farelas, A. Ramirez, *Int. J. Electrochem. Sci*., 5 (2010) 797.
14. Lijuan Feng, Huaiyu Yang, Fuhui Wang, *Int. J. Electrochem. Sci*., 7 (2012) 4064.
15. Shuangkou Chen,Steve Scheiner,Tapas Kar,Upendra Adhikari, *Int. J. Electrochem. Sci.*, 7 (2012) 7128.
16. Luz Maria Rodriguez-Valdez, Alberto Martinez-Villafañe, Daniel Golztman-Mitnik, *Theochem* 713 (2005) 65.
17. K. Bilkova, N. Hackerman, M. Bartos, Proceedings of NACE *Corrosion*/2002, NACE 2002, Denver, CO, paper No. 2284.
18. E. Sosa, R. Cabrera-Sierra, E. Marina, M.E. Rincon, M.T. Oropeza, I. Gonzalez, *Electrochimica Acta* 47 (2002) 1197.
19. H. Ashassi-Sorkhabi, S.A. Nobavi-Amri, *Electrochimica Acta* 47 (2002) 2239.
20. K.G. Gonroy, C.B. Breslin, *Electrochimica Acta* 48 (2003) 721.
21. S :Arzola, J. Mendoza-Florez, R. Duran-Romero, J. Genesca, *Corrosion*, 62 (2006) 433.

22. P.H. Tewart, A.B. Campbell, *Can. J. Chem*., 57 (1979) 188.
23. F.H. Meyer, O.L. Riggs, R.L. McGlasson, J.D. Sudbury, *Corrosion*, 14 (1958) 69.
24. G.W. Walter, *Corros. Sci*., 26 (1989) 681
25. S.H. Yoo, Y. W. Kim, K. W. Chung, S. Y. Baik, J. S. Kim, *Corros. Sci*.,59 (2012) 42.
26. K. Hladky, J.L. Dawson, *Corros. Sci*. 22 (1982) 231.
27. H. Ma, X. Chang, G. Li, S. Chen, Z. Quian, S. Zhao, L. Niu, *Corros. Sci*. 42 (2000) 1669.
28. A J Szyprowski, *Corrosion* 59 (2003) 68.